4-1992

Single and Double Ionization of Helium by Highly Charged Sulfur Ions

Karen M. Lifrieri
Western Michigan University

SINGLE AND DOUBLE IONIZATION OF HELIUM BY HIGHLY CHARGED SULFUR IONS

by

Karen M. Lifrieri

A Thesis
Submitted to the
Faculty of The Graduate College
in partial fulfillment of the
requirements for the
Degree of Master of Arts
Department of Physics

Western Michigan University
Kalamazoo, Michigan
April 1992

SINGLE AND DOUBLE IONIZATION OF HELIUM BY HIGHLY CHARGED SULFUR IONS

Karen M. Lifrieri, M.A.

Western Michigan University, 1992

Single and double ionization of helium by highly charged sulfur projectiles is investigated over an energy range of 0.16 to 1.6 MeV/u. Absolute cross sections for the processes of pure ionization, ionization associated with single capture, and ionization associated with single loss by $S^{6,13+}$ projectiles were experimentally determined and compared with previous results and theories. Ratios of double-to-single ionization for each outgoing projectile charge state were also determined and compared with theory. The pure ionization ratios for S^{6+} at the highest energies investigated show the q^2/E dependence predicted by Knudsen et al. (1984). For S^{13+} the charge and velocity range studied lies outside the perturbative two-step regime so that double ionization cannot be described satisfactorily within the existing theories. Furthermore, it has been found that for both charge states double ionization is significantly enhanced when target ionization is accompanied by projectile electron capture or loss.

ACKNOWLEDGEMENTS

How do you thank the people who have instructed, guided, and shown kindness toward you for the past three years? I tried writing and rewriting my acknowledgement page. Nothing I could write on this one page would be enough to show my gratitude and deep appreciation to my advisor, Dr. John A. Tanis, and the Department of Physics at Western Michigan University, Kalamazoo. To all of you, "Thank You Very Much."

To Fr. Scanlon, Fr. Sesto, my parents, brother, and sisters I thank you with all my heart for being a part of my life.

Finally, I hope that this study will generate some ideas for further investigation in experimental atomic physics.

This work was supported in part by a grant from the U.S. Department of Energy. That support is gratefully acknowledged and appreciated.

Karen M. Lifrieri

Order Number 1347632

Single and double ionization of helium by highly charged sulfur ions

Lifrieri, Karen M., M.A.

Western Michigan University, 1992

U·M·I
300 N. Zeeb Rd.
Ann Arbor, MI 48106

TABLE OF CONTENTS

LIST OF TABLES

LIST OF FIGURES

List of Figures—Continued

CHAPTER I

INTRODUCTION

In this thesis, atomic collisions between ionized projectiles and neutral target atoms are investigated. Studies of atomic collision processes are important as they can lead to a better understanding of fundamental atomic interactions as well as an understanding of applied phenomena such as charge transfer in the ionosphere, the characteristics of astrophysical and fusion plasmas, and laser technology (Harrison, 1978; Hogan, 1978; Gilbody, 1979; Janev, 1989). For example, the current generation, as well as the next generation of tokamak-type fusion reactors, requires a knowledge of the cross sections obtained from ion-atom collisions. Furthermore, the study of ion-atom collisions can help theorists to find appropriate approximations to the many-body problem.

During a collision between an ionized projectile and a neutral target atom, processes of excitation, charge transfer, and ionization can occur. When a projectile ion or target atom experiences excitation during a collision, an electron undergoes a transition from its initial energy level to a higher level. This excited state is unstable and the electron returns to its initially unexcited state via photon emission or Auger electron emission. For charge-changing processes, the projectile can capture or lose electrons while the target can become singly, doubly, or

multiply ionized. Single ionization is well understood both theoretically and experimentally, and is adequately described in the framework of the first Born approximation (Inokuti, 1971; Shah & Gilbody, 1981; McGuire, Muller, Schuch, Groh, & Salzborn, 1987). Ionization processes involving more than one electron are less well understood. Methods such as the independent electron model (IEM) are used to describe these multielectron processes (McGuire & Weaver, 1977). In this model, the target atom is treated as a collection of electrons which independently interact with the projectile, i.e., electron-electron interactions are ignored.

The purpose of this thesis is to investigate experimentally the mechanisms leading to double ionization at intermediate velocities, i.e., $v_{projectile} \lesssim 10\ v_{Bohr}$. Through experimental investigation and comparison with theory, we can check whether double ionization can be interpreted in the framework of the IEM and also study the electron-electron interaction. Measurements of single and double ionization of helium by S^{6+} and S^{13+} projectiles were made. Helium was chosen as the target atom because it is the simplest multielectron atom and double ionization can be unambiguously identified. The projectile ion energy range was 5-35 MeV and 15-50 MeV for S^{6+} and S^{13+}, respectively. By using two different charge states over this energy range, information can be obtained about how the velocity and projectile charge state influence double ionization. Additionally, S^{13+} is a tightly bound "pointlike" projectile, while S^{6+} is a larger, less tightly bound ion for which its spatial extent may come into play.

Previous measurements of single-electron capture and loss by S^{13+} projectiles incident on He were made by Clark et al. (1986); however, the final ionization state of the target was not determined. Measurements of the double ionization of helium related to those conducted here include those of Heber, Bandong, Sampoll, and Watson (1990) using N^{7+} for the projectile and Tanis, Bernstein, Clark, Ferguson, and Price (1991) using $O^{6,7+}$ for the projectile.

For the collision systems considered here, single and double target ionization can occur via (a) pure ionization in which the final charge state of the projectile is left unchanged, (b) associated single-electron capture by the projectile, and (c) associated single-electron loss from the projectile. In this work, cross sections for the single and double ionization of helium were determined for each of these cases. The ratio R of double-to-single ionization was also determined. This ratio is important because it contains basic information on the mechanisms responsible for double ionization. The measured ratios were compared with theoretical predictions. Absolute cross sections for single and double ionization are compared with previous results and theories.

CHAPTER II

THEORY

In this work, we are interested in the single and double ionization of helium target atoms accompanied by single-electron capture, single-electron loss, or no charge change by incident S^{6+} and S^{13+} projectiles. Although S^{13+} is not a bare ion, the three electrons in the K and L shells are tightly bound so that the projectile can be considered (almost) a point particle. On the other hand, S^{6+} is a much larger, many-electron atom for which the atomic structure is probably significant. By studying single and double ionization of He by these ions over an energy range of 5-50 MeV, we are able to obtain information about the projectile velocity and charge dependence of the ionization process.

For the collision systems studied here, six charge-changing processes are possible.

$$S^{q+} + He \text{ ------> } S^{(q-1)+} + He^{+} \quad (1a)$$

$$\text{ ------> } S^{(q-1)+} + He^{++} + e^{-} \quad (1b)$$

$$S^{q+} + He \text{ ------> } S^{(q+1)+} + He^{+} + 2e^{-} \quad (2a)$$

$$\text{ ------> } S^{(q+1)+} + He^{++} + 3e^{-} \quad (2b)$$

$$S^{q+} + He \text{ ------> } S^{q+} + He^{+} + e^{-} \quad (3a)$$

$$\text{ ------> } S^{q+} + He^{++} + 2e^{-} \quad (3b)$$

Reactions 1, 2, and 3 correspond to single and double ionization of the target associated with single-electron capture, single-electron loss and no charge change by the projectile. Throughout this thesis, the notation used to denote the cross section for the above mentioned reactions is as follows: $\sigma^{0i}_{q,q-1}$, $\sigma^{0i}_{q,q+1}$, $\sigma^{0i}_{q,q}$ i=1,2, where the subscript refers to the initial and final charge states of the projectile while the superscript refers to the initial and final charge states of the target atom.

Of particular interest in this work is the double ionization of helium to determine the nature of the interaction(s) leading to the ejection of two electrons in a single collision. It has been proposed (McGuire, 1982) that the double ionization of helium can occur through two processes: shakeoff (SO) and two-step (TS).

In the shakeoff mechanism, one electron is ejected to the continuum through a direct interaction between the projectile nucleus and a target electron; and a second electron is "shaken off" as a result of the electron-electron interaction in the initial state of the He target atom. That is, the ejection of the first electron causes a rearrangement of the electron cloud thereby leading to the ejection of the second electron (McGuire, 1984). Since this process is due to a single encounter between the projectile nucleus and a target electron, the cross section for this shakeoff process is proportional to the single ionization cross section, i.e., σ_{SO} = constant x σ^{01}. The cross section for single ionization by charged particles is understood in terms of the Born approximation (Inokuti, 1971; Madison & Merzbacher, 1972) and varies as $(q/v)^2\ln(v)$ where v and q are the projectile velocity and charge. Thus, we can write:

$$\sigma_{SO} = \text{constant x } (q/v)^2 \ln(v) \tag{4}$$

where the ln(v) term comes from integration over the tail of the long-range Coulomb potential of the projectile (Inokuti, 1971).

Unlike the shakeoff mechanism, the two-step process results from two separate interactions between the projectile nucleus and the target electrons. That is, each target electron is liberated via a single encounter between the projectile and the target (see Figure 1). Thus, the cross section for double ionization due to the two-step mechanism (McGuire, 1982) in the first Born approximation is given by the square of the single ionization cross section, i.e.,

$$\sigma_{TS} = \text{constant x } (q/v)^4. \tag{5}$$

It should be noted that McGuire (1982) found the two-step cross section independent of the ln(v) term due to a relatively large momentum transfer in the double ionization process. Furthermore, the ln(v) term is important only at relativistic velocities (Inokuti, 1971).

Quantum mechanically we express the double ionization cross section as the square of a sum of probability amplitudes, that is,

$$\begin{aligned} \sigma^{02} &= \sum |A_{SO}(q/v) - A_{TS}(q/v)^2|^2 \\ &= \sigma_{SO} - \sigma_{INTF} - \sigma_{TS} \end{aligned} \tag{6}$$

where σ_{INTF} is the cubic cross term resulting from interference between the shakeoff and two-step mechanisms.

A way of investigating the mechanisms involved in the double ionization of

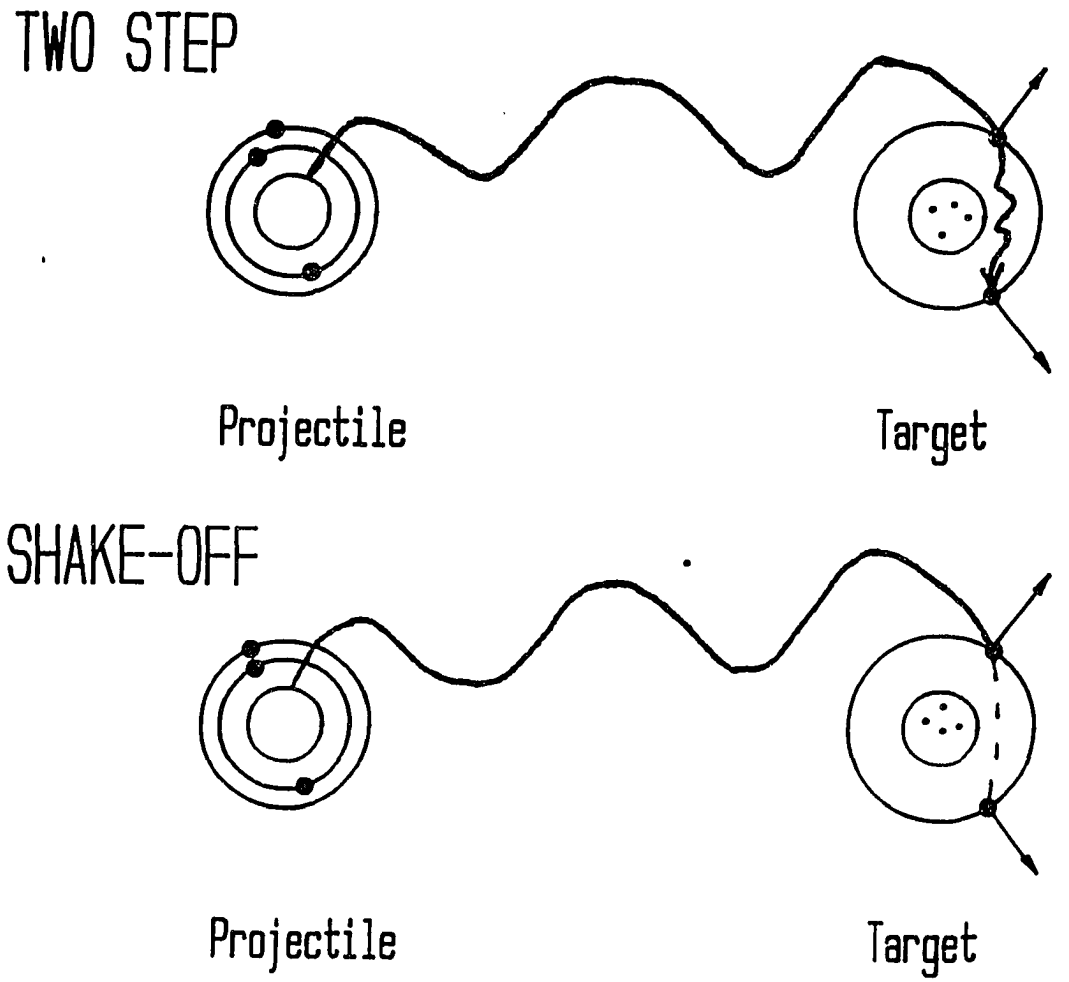

Figure 1. Diagram of the Two-Step and Shakeoff Mechanisms for Double Ionization.

helium is through the ratio R of double-to-single ionization. From the description above, this ratio is given by

$$R = \frac{\sigma^{02}}{\sigma^{01}} = \frac{\sigma_{SO} + \sigma_{INTF} + \sigma_{TS}}{\sigma^{01}}$$

$$= C_{SO} + C_{INTF} \times \frac{q}{v} + C_{TS} \times \left(\frac{q}{v}\right)^2 \qquad (7)$$

where the ln(v) term has been omitted since it should not be important for the projectile velocities considered here. Thus, for shakeoff this ratio is independent of the projectile velocity and approaches a constant value (C_{SO}) at high velocities, whereas in the intermediate velocity region where the two-step mechanism dominates, R varies as $(q/v)^2$. For velocities where both mechanisms are of comparable magnitude, the interference term may also become significant.

Briefly reiterating, C_{SO} is a constant term resulting from a single projectile-target interaction; the last term is associated with double ionization by two separate direct interactions; and the middle term in Eq. (7) stems from an interference between these two competing mechanisms.

Knudsen et al. (1984) obtained values for the constants in Eq. (7) by fitting data for R for fully-stripped ions. These authors obtained the following expression for R

$$R = 2.20\times10^{-3} + 4.55\times10^{-3}\frac{q^2}{E\ln(13.12\sqrt{E})} \qquad (8)$$

where E is measured in MeV/amu. This semi-empirical expression was determined for 0.13-15 MeV/amu projectile ions with incident charges ranging from 1-8. In

Chapter IV, the R values obtained in this work for S^{6+} and S^{13+} ions incident on helium targets will be compared with the predictions of this semi-empirical result.

CHAPTER III

EXPERIMENT

Apparatus

This experiment was performed on a 6 MV EN tandem Van de Graaff accelerator at Western Michigan University, Kalamazoo, shown schematically in Figure 2. Negative sulfur ions were produced by placing iron sulfide in a sputter ion source. These ions were extracted and injected into the accelerator. Inside the accelerator, the negative ions get accelerated to the positive terminal which can be charged up to a maximum of six million volts. At the high voltage terminal, the negative ions pass through a thin (typically 10 $\mu g/cm^2$) carbon foil. This foil removes the loosely bound outer-shell electrons thereby making positive sulfur ions. These positive ions get repelled and further accelerated by the high positive charge on the terminal. The beam is focused and charge analyzed by a 90° bending magnet which selects the desired energy and charge state, following which the beam is directed to the appropriate beam line by a switching magnet. In the beam line, the beam was collimated by two sets of slits located approximately 1.5 meters apart. The pressure in the beam line was typically around 10^{-6} torr, as maintained by oil diffusion pumps.

The beam then entered the target region (see Figure 3). For this

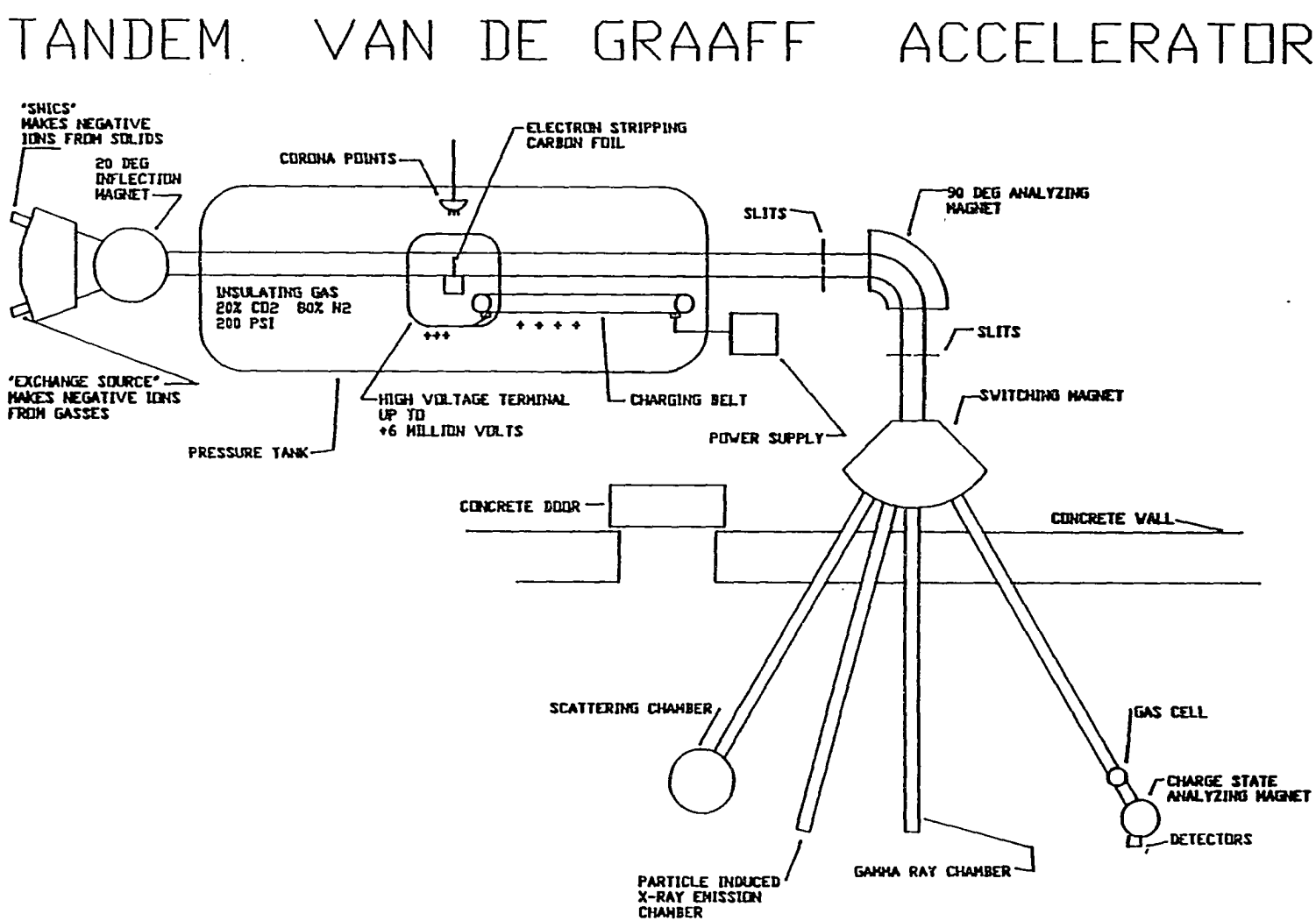

Figure 2. Schematic of the 6 MV EN tandem Van de Graaff Accelerator at Western Michigan University.

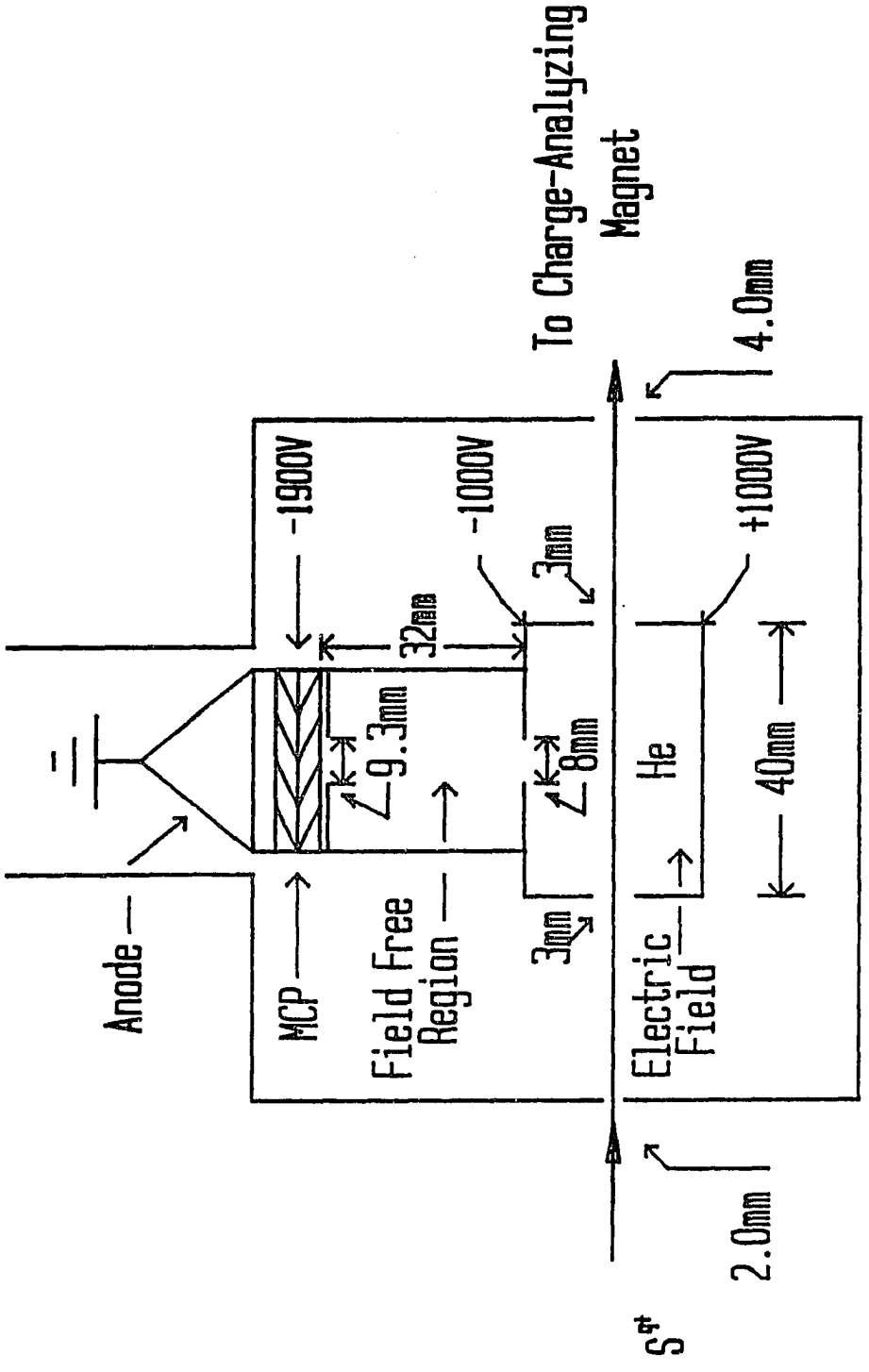

Figure 3. Schematic of Target Region and Recoil Detector.

experiment, the target region consisted of a differentially pumped gas cell with entrance and exit apertures of 3.00 mm diameter. The entrance and exit apertures to the differential pumping section were 2.00 mm and 4.00 mm respectively. The pressure inside the gas cell was monitored by a capacitance manometer system, and was varied during an experimental run from 0 to 0.5 mTorr.

Inside the target region, sulfur ions underwent collisions with neutral helium target atoms. The helium recoil ions produced in the collision were extracted perpendicular to the projectile beam direction through a potential difference of 2000 V. Once extracted, the recoil ions travelled through a field-free region. The total time of flight in the field-free region was approximately 160 ns and 110 ns, for the He^{+} and He^{++} ions, respectively. After exiting the field-free region, the helium ions struck a negatively biased microchannel plate. Meanwhile, sulfur ions exiting the gas cell were bent by a charge-state analyzing magnet and detected by solid-state detectors. The component of the beam that did not change charge was collected in a Faraday cup as shown in Figure 4. Coincidences were detected between the helium recoil ions and projectile ions that gained or lost electrons.

Electronics

During this experiment, two different types of measurements, known as "singles" and coincidence, were made. For a "singles" run, we measured only projectile ions that gained or lost electrons without observing He recoil ions, while

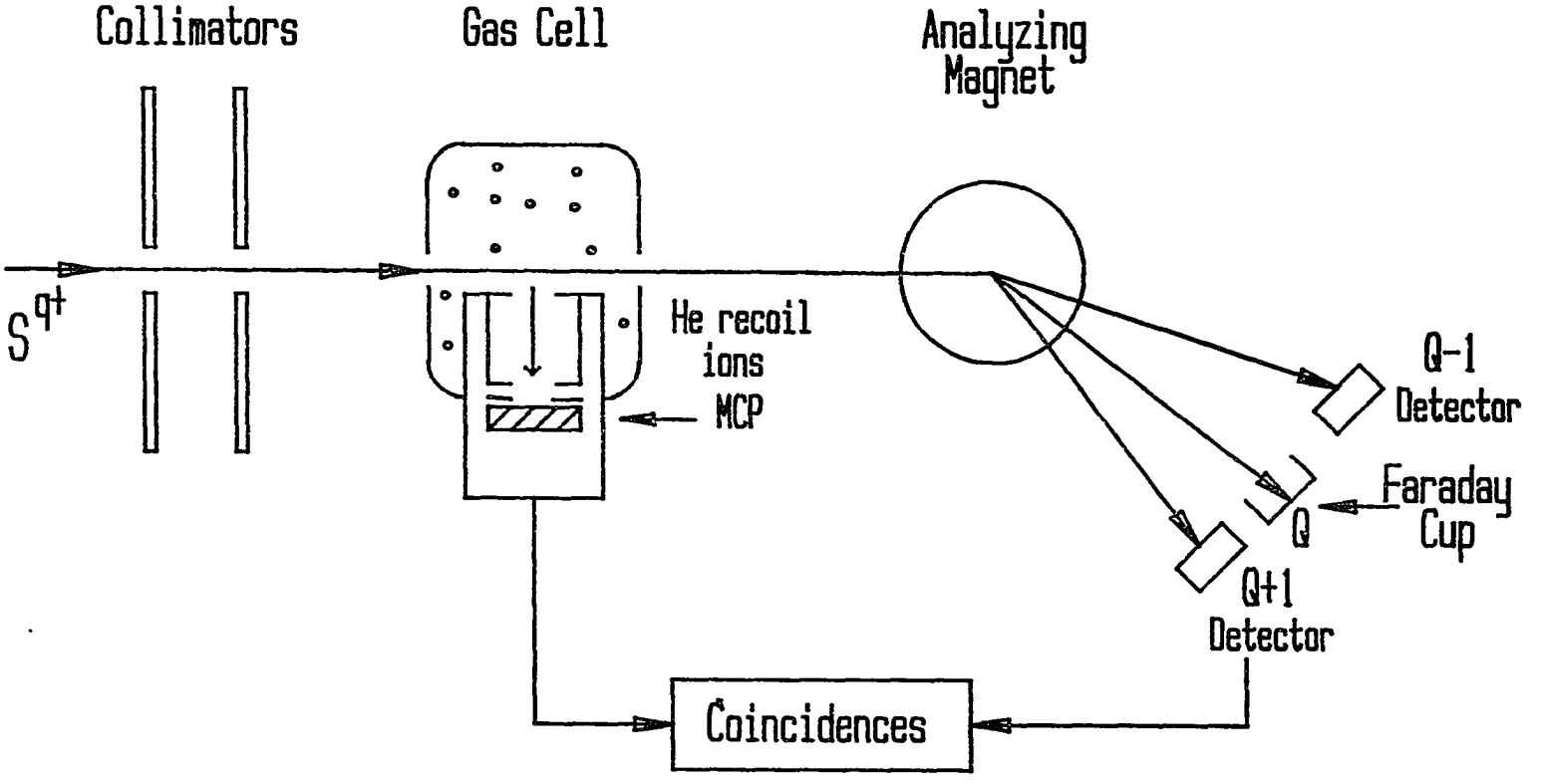

Figure 4. The Atomic Physics Beamline at Western Michigan University.

the coincidence measurements recorded He target recoil ions associated with projectiles capturing or losing electrons. In both cases, the unchanged charge component of the incident beam was collected in a Faraday cup. In separate measurements, coincidences between the unchanged charge component of the projectile beam and recoil target ions were also detected. This was done by replacing the Faraday cup with a surface-barrier detector and reducing the incident beam intensity. See Figures 5 and 6 for a schematic of the electronics.

For the "singles" measurements, charge-changed projectile ions struck the surface barrier detectors and produced a signal. This signal was amplified by a pre-amplifier and a timing filter amplifier (TFA) and then sent to a constant fraction discriminator (CFD). The discriminator was set to reject noise pulses below about 0.05 V. The CFD produces a logic signal output indicating that an ion has been detected, and this event was then recorded on a counter (scaler).

The other type of measurement involved the detection of coincidences between projectile ions in a specific charge state and recoiling He target ions. The helium recoil ions were charge analyzed by their flight time. These recoil ions were extracted by a static electric field and, after traveling through a field-free region, were detected by a negatively biased microchannel plate. Since the time-of-flight of the recoil ion (He^{+} or He^{++}) is proportional to the inverse square root of its charge, the charge of the recoil ion is determined by its time-of-flight.

The detected recoil ions produced a signal that was sent to a fast timing amplifier (FTA), a timing filter amplifier (TFA), and then to a constant fraction

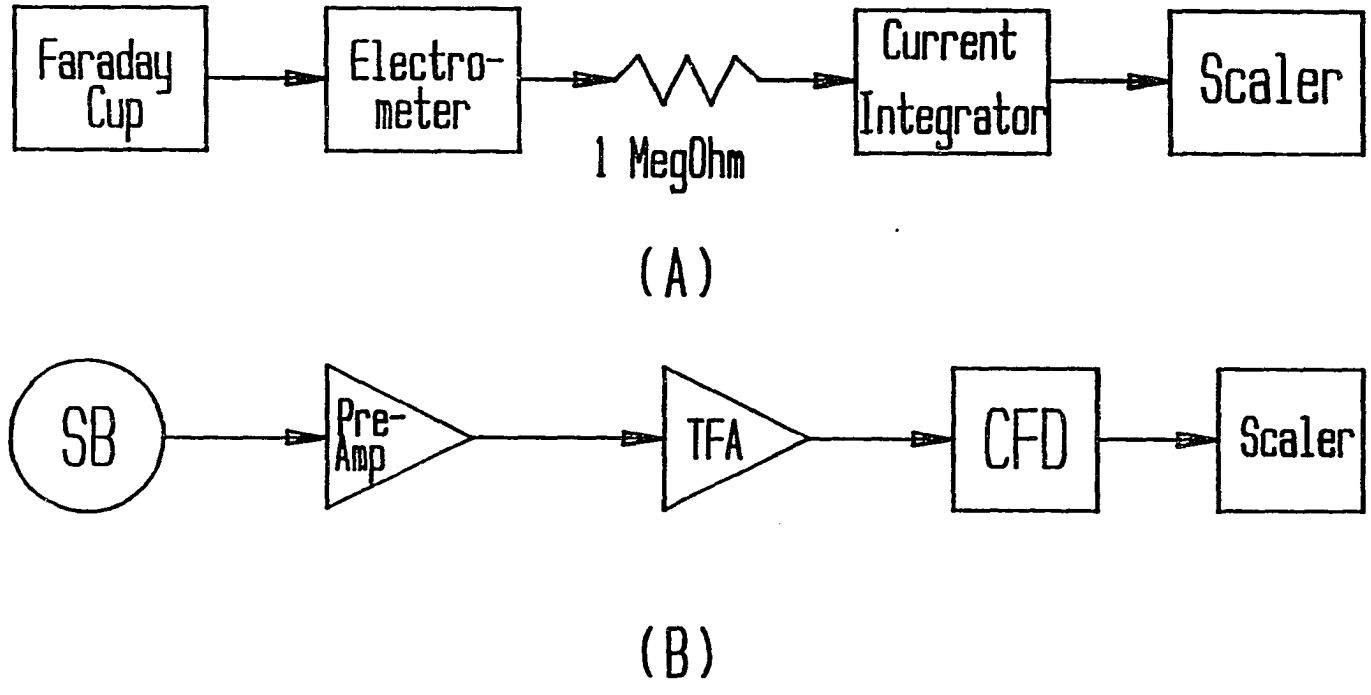

Figure 5. Diagram of Electronics Used During Singles Measurements.
(a) Electronics Used to Measure the Unchanged Charge Component of the Projectile Beam.
(b) Electronics Used During the Singles Measurements.
Key to abbreviations: SB - Surface Barrier Detector TFA - Timing Filter Amplifier CFD - Constant Fraction Discriminator.

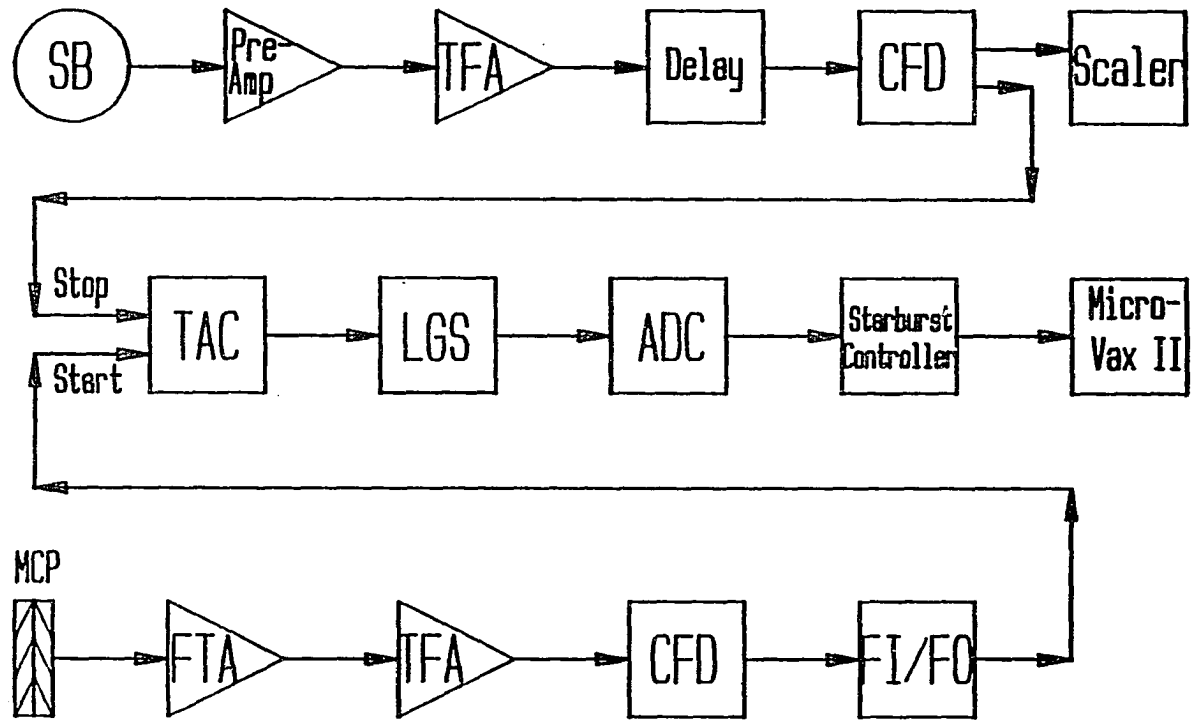

Figure 6. Diagram of Electronics Used During Coincidence Measurements. Key to abbreviations: SB - Surface Barrier Detector TFA - Timing Filter Amplifier CFD - Constant Fraction Discriminator TAC - Time-to-Amplitude Converter LGS - Linear Gate Stretcher ADC - Analog-to-Digital Converter FI/FO - Fan In/Fan Out FTA - Fast Timing Amplifier.

discriminator (CFD). The negative logic output of the CFD was routed through a fan in/fan out (FI/FO) which provided the START for a time-to-amplitude converter (TAC). The signals from the charge-changed projectile ions striking the surface-barrier (SB) detector were delayed by about 100 ns before going to the constant fraction discriminator. The CFD output then provided the STOP signal for the TAC.

The TAC outputs an analog signal whenever a START and a STOP are received within the preselected full-scale time range used (2 μsec in this case). Since the amplitude of this output signal depends on the time difference between the START and STOP pulses, the amplitude of the signal determines the charge of the recoiling target ion. The signal from the TAC was sent through a linear gate stretcher (LGS), and then to an analog-to-digital converter (ADC). The ADC output was interfaced to a MicroVAX 2 computer using a Starburst interface module. The digital information obtained was then processed by the data acquisition program CHAOS.

The unchanged charge component of the incident beam was collected in a Faraday cup (see Figure 5) which was connected to a Keithley electrometer. The electrometer gave a 2-volt output for a full-scale input reading. This voltage was converted to a current by "dropping" it across a 1 MΩ resistor, and then input to a beam current integrator. The integrator digitized the current to enable determination of the total charge collected by the Faraday cup, and in turn, the total number of incident particles.

Typical spectra for projectile single-electron capture and loss events coincident with single and double ionization of the helium target atoms are shown in Figure 7. The small peak located at the far right results from the detection of photons (or zero time).

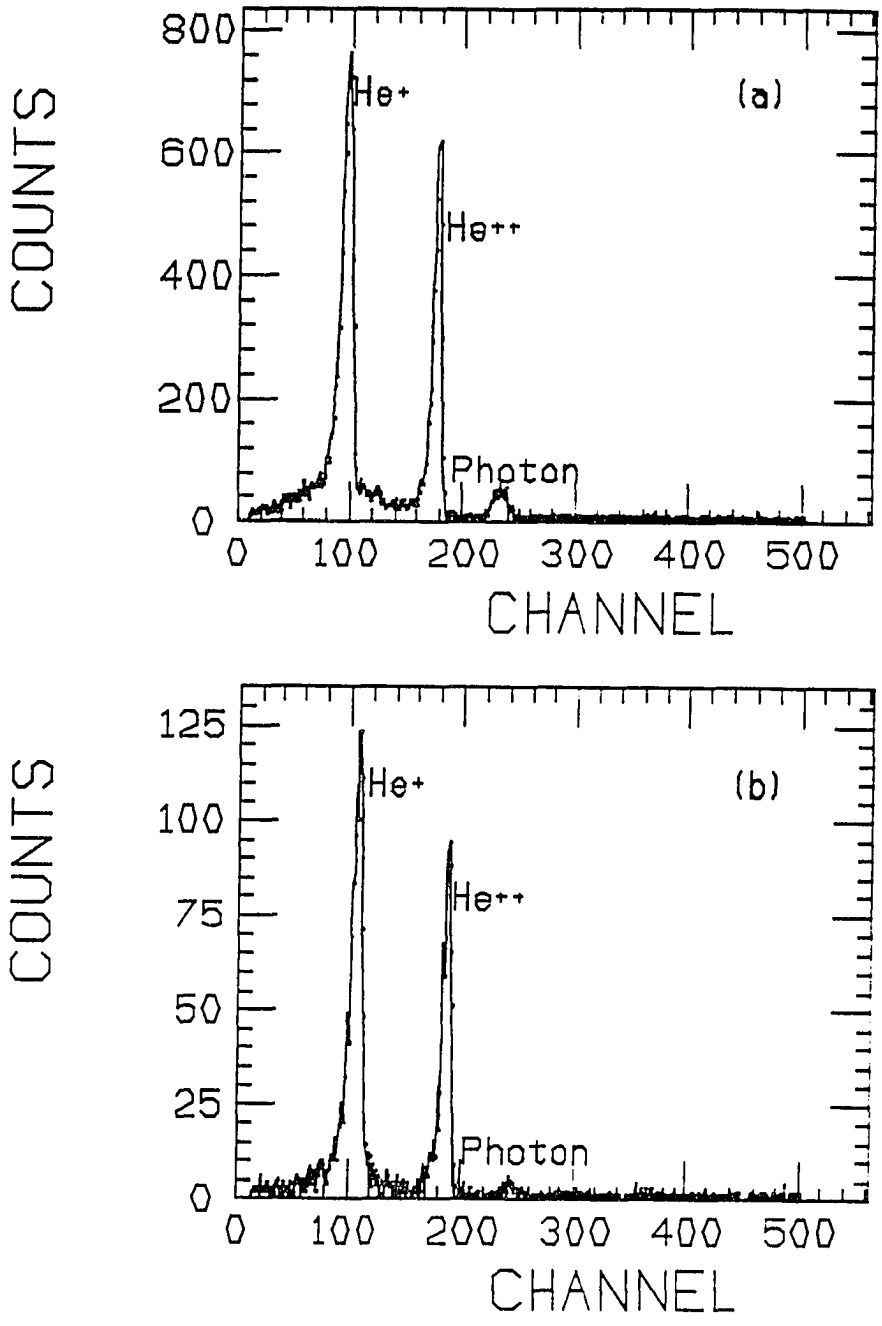

Figure 7. Typical Recoil-Ion Time-of-Flight Spectra for 50 Mev S^{13+} on He. The top spectrum (a) shows single electron capture. The lower spectrum (b) shows single electron loss.

CHAPTER IV

DATA ANALYSIS AND RESULTS

Determination of Cross Sections

For each experimental run at a particular beam energy and charge state, the target gas cell pressure was varied. Typically, measurements were made at pressures of 0, 0.3 and 0.5 mTorr. A run was also done without any beam to correct for offset in the meter used to measure the incident beam current. Then for each energy, charge state, and pressure, the fraction of detected particles or coincidence events compared to the total number of incident particles was determined, i.e.,

$$F = \frac{N_d}{N_{tot}} \tag{9}$$

where N_d = number of events of interest and N_{tot} is the total number of incident particles. But, $N_{tot} = N_Q + N_{Q-1} + N_{Q+1}$, where $N_{Q\pm1}$ are projectile ions that gained or lost an electron, and N_Q represents ions that did not change charge. The fraction F was plotted as a function of gas pressure (see Figure 8) to check for linearity, thus ensuring that single-collision conditions prevailed inside the gas cell. From the slope of this line ($\Delta F/\Delta P$), the cross section (σ) for the process of interest was then determined.

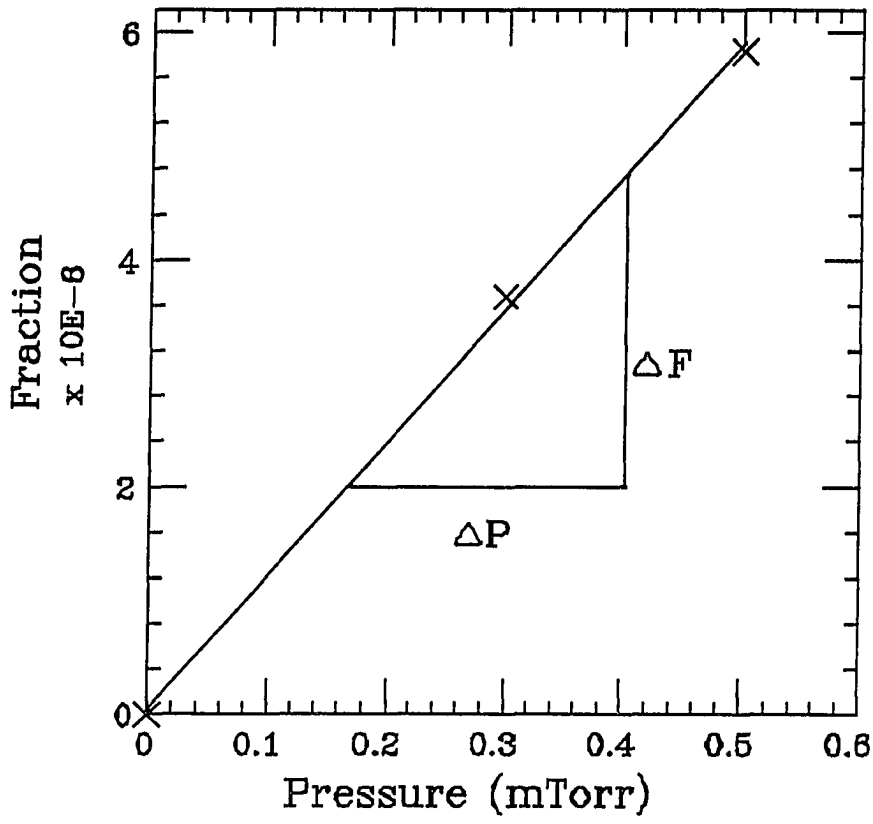

Figure 8. Fraction Versus Pressure for Single-Electron Capture in Coincidence With Single Ionization of the Target for 25 MeV S^{13+} + He.

Now, the number of detected particles or coincidence events in Eq. (9) is given by

$$N_d = N_{tot}\sigma T\varepsilon \tag{10}$$

where σ is the cross section in cm^2, ε is the detector efficiency, and T is the target thickness in atoms/cm^2. The target thickness (T) is given by

$$T = N_o PL \tag{11}$$

where $N_o = 3.3x10^{13}$ atoms/mTorr cm^3, P is the gas pressure in mTorr, and L is the length of the gas cell in cm. Combining Eqs. (9), (10) and (11) then gives

$$\sigma = \frac{(\Delta F/\Delta P)}{N_o L\varepsilon}. \tag{12}$$

Thus, the importance of the slope from the graph of fraction vs. pressure is evident, i.e., from the slope and constants which are known or can be measured, the experimental cross sections are determined.

The uncertainties in the cross sections can be attributed to the length of the gas cell (<5%), calibration of the Keithley electrometer (<5%), pressure fluctuations in the gas cell (<4%), and error from fitting a straight line to the fractional yield vs. pressure data (<10%). From these individual sources of error, the total uncertainties in the cross sections were found by combining the individual errors in quadrature. This gave an overall absolute uncertainty in the coincidence cross sections of ±13%.

Single-Electron Capture and Loss Cross Sections

Single electron capture and loss cross sections for S^{6+} and S^{13+} incident on helium are listed in Table 1 along with their relative uncertainties. Figures 9 and 10 show these single-electron capture and loss cross sections plotted as a function of energy. The solid curve (electron capture) is the empirical scaling rule of Schlachter et al. (1987) given by

$$\tilde{\sigma} = \frac{3.52\times10^{-9}(1-e^{(-0.083\tilde{E}^{1.33})})\times(1-e^{(-7.5\times10^{-4}\tilde{E}^{2.45})})}{\tilde{E}^{(4.18)}}$$

$$\tilde{\sigma} = \frac{\sigma Z^{1.8}}{q^{0.7}}$$

and

$$\tilde{E} = \frac{E}{Z^{1.25}q^{0.5}}$$

where q is the charge of the projectile, Z is the atomic number of the target, and E is the projectile kinetic energy in keV/u. The dot-dash curve (electron loss) was generated from calculations of Choi, Merzbacher, and Khandelwal (1973), and is based on the plane-wave Born approximation (PWBA). Also shown with the S^{13+} data are the measurements of Clark et al. (1985).

It is seen that the capture cross sections for both S^{6+} and S^{13+} decrease by at least two orders of magnitude over the energy range considered, while the loss cross sections are much less dependent on energy. The S^{6+} electron capture data all lie beneath the calculated curve. The S^{13+} capture data, however, are in good

Table 1

Cross Sections for Single-Electron Capture and Loss
for S^{6+} and S^{13+} Projectiles Colliding
With Helium Target Atoms

E (MeV)	$\sigma_{q,q-1}$ (cm^2)	$\sigma_{q,q+1}$ (cm^2)
	q = 6+	
10	(6.7 ± 0.7) [-17]	(1.3 ± 0.1) [-17]
15	(1.6 ± 0.2) [-17]	(1.4 ± 0.1) [-17]
20	(4.5 ± 0.5) [-18]	(1.6 ± 0.2) [-17]
25	(2.5 ± 0.3) [-18]	(1.5 ± 0.2) [-17]
30	(1.3 ± 0.1) [-18]	(1.6 ± 0.2) [-17]
35	(6.3 ± 0.6) [-19]	(1.3 ± 0.1) [-17]
40	(3.7 ± 0.4) [-19]	(1.3 ± 0.1) [-17]
	q = 13+	
15	(2.1 ± 0.2) [-16]	(1.2 ± 0.1) [-19]
20	(7.6 ± 0.8) [-17]	(2.5 ± 0.3) [-19]
25	(3.7 ± 0.4) [-17]	(3.5 ± 0.4) [-19]
30	(2.1 ± 0.2) [-17]	(4.1 ± 0.4) [-19]
40	(6.0 ± 0.6) [-18]	(4.1 ± 0.4) [-19]
50	(2.4 ± 0.2) [-18]	(4.1 ± 0.4) [-19]
55	(1.6 ± 0.2) [-18]	(4.1 ± 0.4) [-19]
58	(1.3 ± 0.1) [-18]	(4.1 ± 0.4) [-19]

Absolute uncertainties in the measured cross sections are less than ± 15%.

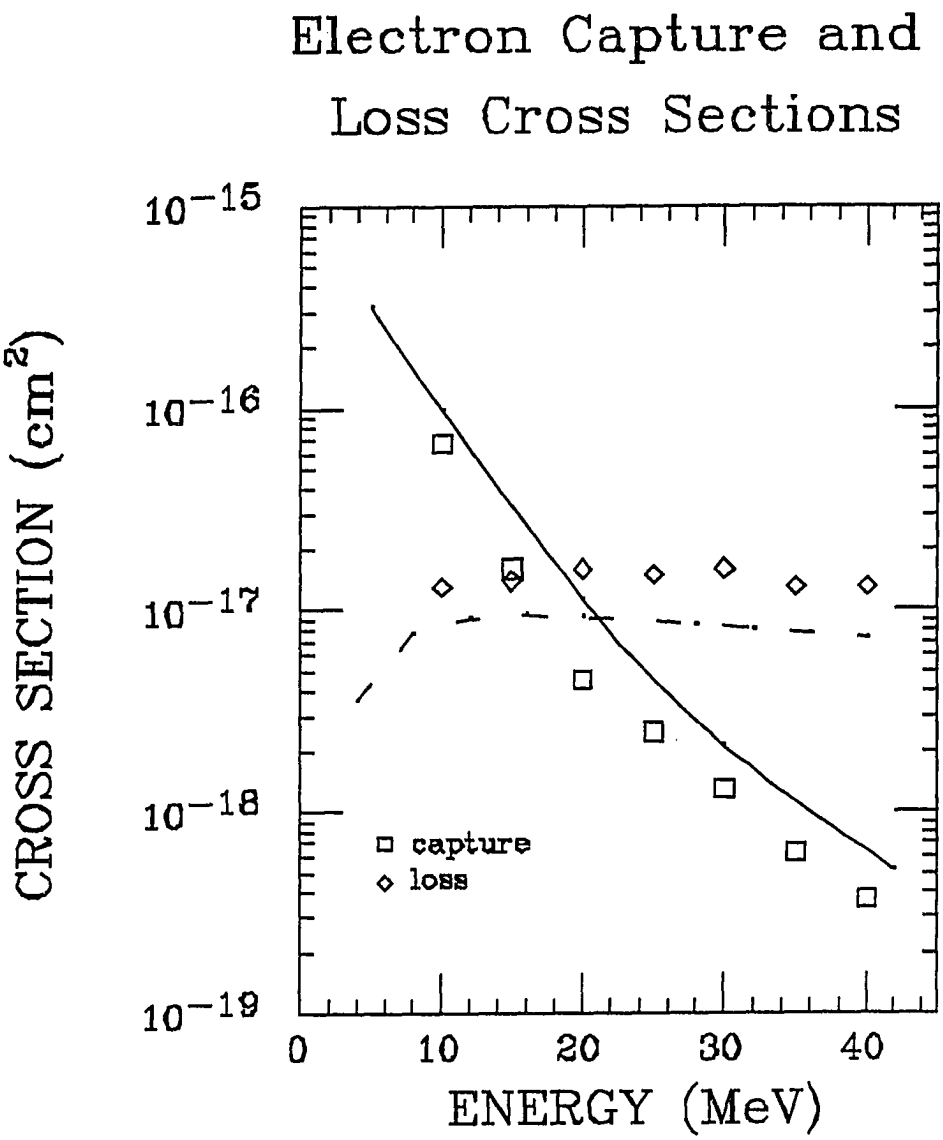

Figure 9. Cross Sections for Electron Capture and Loss for S^{6+} + He. The solid curve is the empirical scaling rule of Schlachter et al. (1987). The dot-dash curve was generated from the PWBA calculations of Choi et al. (1973).

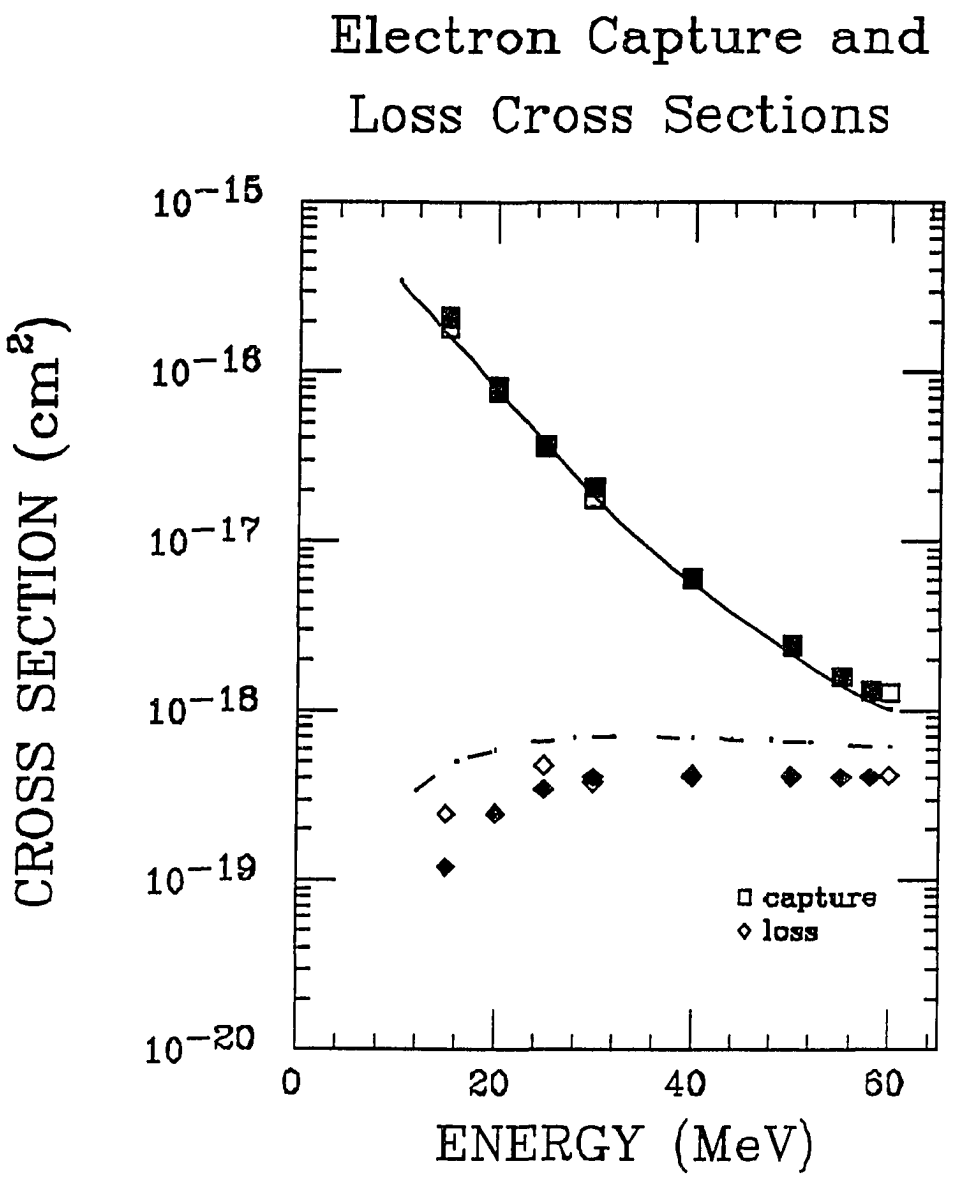

Figure 10. Cross Sections for Electron Capture and Loss for S^{13+} + He. The solid curve is the empirical scaling rule of Schlachter et al. (1987). The dot-dash curve was generated from the PWBA calculations of Choi et al. (1973). The solid symbols represents present data. The open symbols are from Clark et al. (1985).

agreement with the empirical scaling curve of Schlachter et al. (1987), and are also in good agreement with the data of Clark et al. (1985). Theory and experiment for the S^{6+} loss cross sections disagree by about 20% with the experimental values being above the theory. The measured loss cross sections for S^{13+}, which are in agreement with those of Clark et al. (1985), lie on average 20% below the Born cross sections.

Ratios of Double-to-Single Ionization

Also determined was the ratio R of double-to-single ionization. This ratio was computed at a particular energy simply by summing the measured intensities (see Fig. 7) of the doubly- and singly-ionized helium recoil ions and then dividing. These ratios are listed in Table 2 for target ionization accompanied by projectile electron capture, target ionization accompanied by projectile electron loss, and pure target ionization (no projectile charge change).

In Figures 11 and 12, the pure ionization ratios for S^{6+} and S^{13+} are plotted as a function of energy. For both charge states, these pure ionization ratios are all smaller than 20%. Also shown are the ratios for target ionization associated with projectile electron capture or loss. For the energy range considered, the ratios are greatest when target ionization is accompanied by projectile electron capture with R reaching values in excess of unity for both q = 6+ and q = 13+. Thus, the ratios are greatly enhanced when target ionization is accompanied by projectile electron capture or loss. A possible explanation for this (Tanis et al., 1991) is that

Table 2

Ratios of Double-to-Single Ionization of Helium in Coincidence With Projectile Electron Capture, Electron Loss, and No Charge Change by S^{6+} and S^{13+} Ions

E (MeV)	$R_{q,q-1}$	$R_{q,q+1}$	$R_{q,q}$
		q = 6+	
5	0.57 ± 0.01	0.36 ± 0.02	0.13 ± 0.01
10	0.89 ± 0.01	0.69 ± 0.01	0.15 ± 0.01
20	0.92 ± 0.01	0.69 ± 0.01	0.10 ± 0.01
25	1.03 ± 0.02	0.60 ± 0.01	0.09 ± 0.01
35	0.97 ± 0.03	0.55 ± 0.01	0.07 ± 0.01
		q = 13+	
15	1.02 ± 0.02		0.18 ± 0.01
20	1.10 ± 0.05	0.77 ± 0.06	0.19 ± 0.01
25	0.99 ± 0.07	0.93 ± 0.07	0.19 ± 0.01
30	0.89 ± 0.04	0.88 ± 0.04	0.17 ± 0.01
40	0.70 ± 0.06	0.68 ± 0.03	0.14 ± 0.01
50	0.50 ± 0.04	0.53 ± 0.02	0.13 ± 0.01

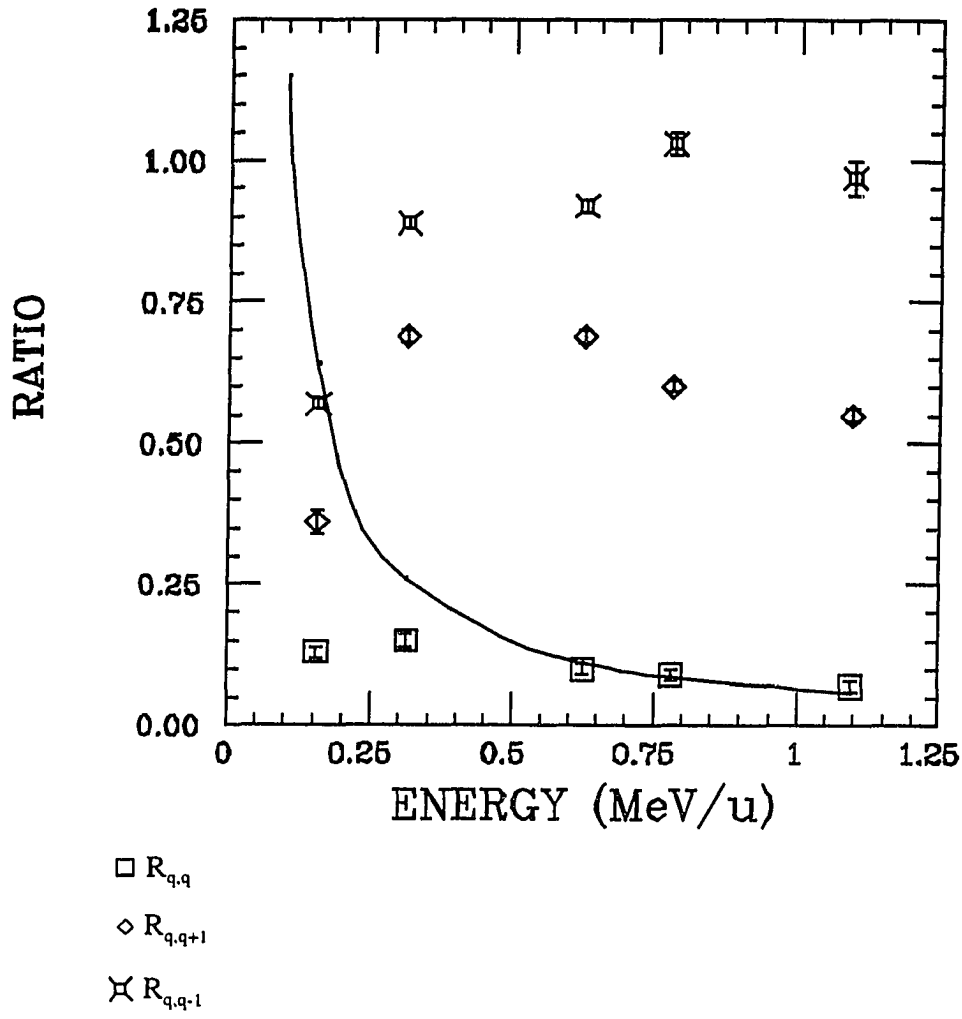

Figure 11. Ratios of Double-to-Single Ionization of He for S^{6+} + He Collisions. The solid curve represents the scaling of Knudsen et al. (1984) given by Eq. 8.

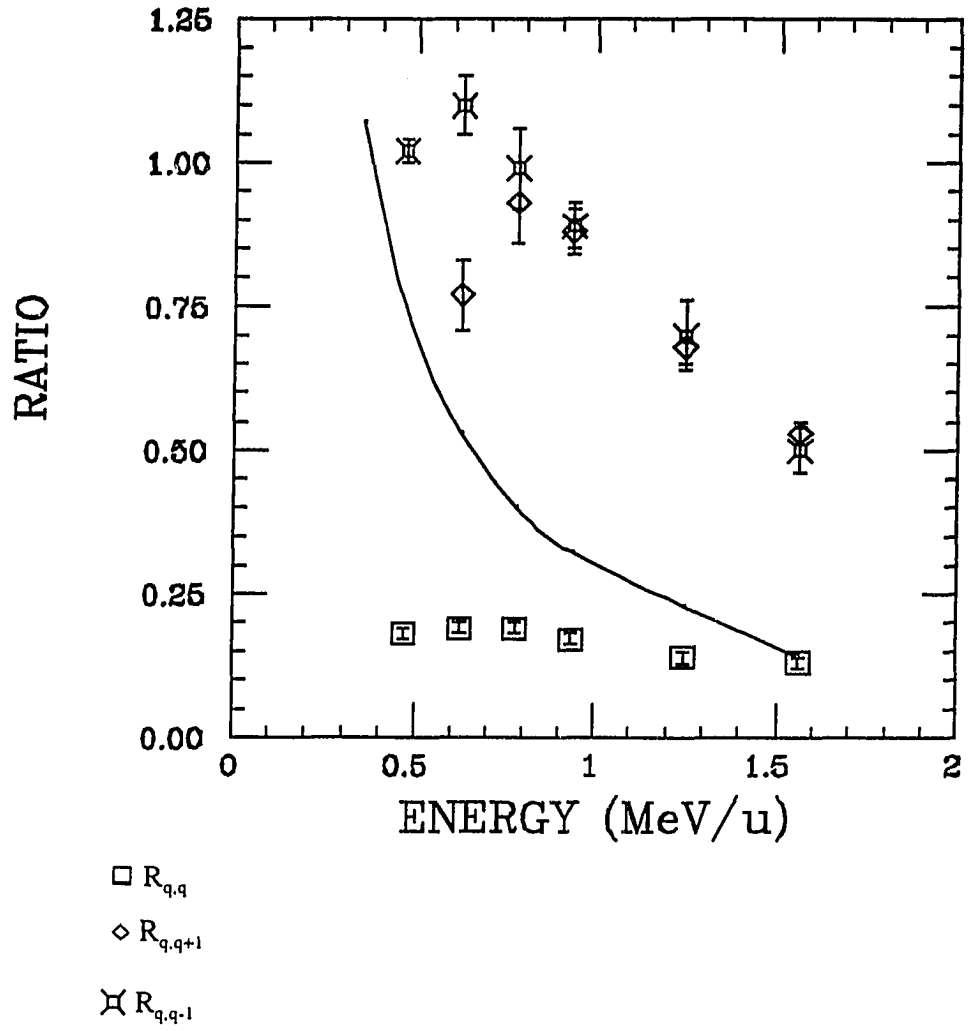

Figure 12. Ratios of Double-to-Single Ionization of He for S^{13+} + He Collisions. The solid curve represents the scaling of Knudsen et al. (1984) given by Eq. 8.

target ionization accompanied by projectile electron capture or loss events are restricted to a limited range of small impact parameter collisions, while target ionization associated with no projectile charge change occurs for relatively large impact parameters.

The solid curves in Figures 11 and 12 were generated from Eq. (8) (see Chapter II). The first term in this equation is dominant for high projectile velocities (Knudsen et al., 1984). Since the present data fall well below the high-velocity region, this constant term is unimportant. The second term in Eq. (8) is valid in the perturbative two-step regime, i.e., $0.2 \lesssim \frac{q}{v} \lesssim 0.5$ (Knudsen et al., 1984). The S^{13+} data are outside this region and hence do not follow the predicted curve as expected. For q = 6+, the data converge with the theory at the highest energy points, however.

According to Eq. (8), R should be a linear function of $q^2/E \ln(13.12\sqrt{E})$ and in Figures 13 and 14, R is plotted as a function of this parameter. It can be seen that only the S^{6+} pure ionization ratios at the highest energies agree with the predicted curve. For both charge states, the ratios for target ionization accompanied by projectile electron capture or loss do not follow the predicted q^2/E dependence at all.

Plotted in Figure 15 are the pure ionization ratios for q = 6+ and 13+ as a function of velocity (in a.u.) divided by the charge. For S^{6+} v/q ranges from 0.4-1.1 while S^{13+} has a v/q range of 0.3-0.6. The TS line denotes the v^{-2} velocity dependence of the two-step mechanism.

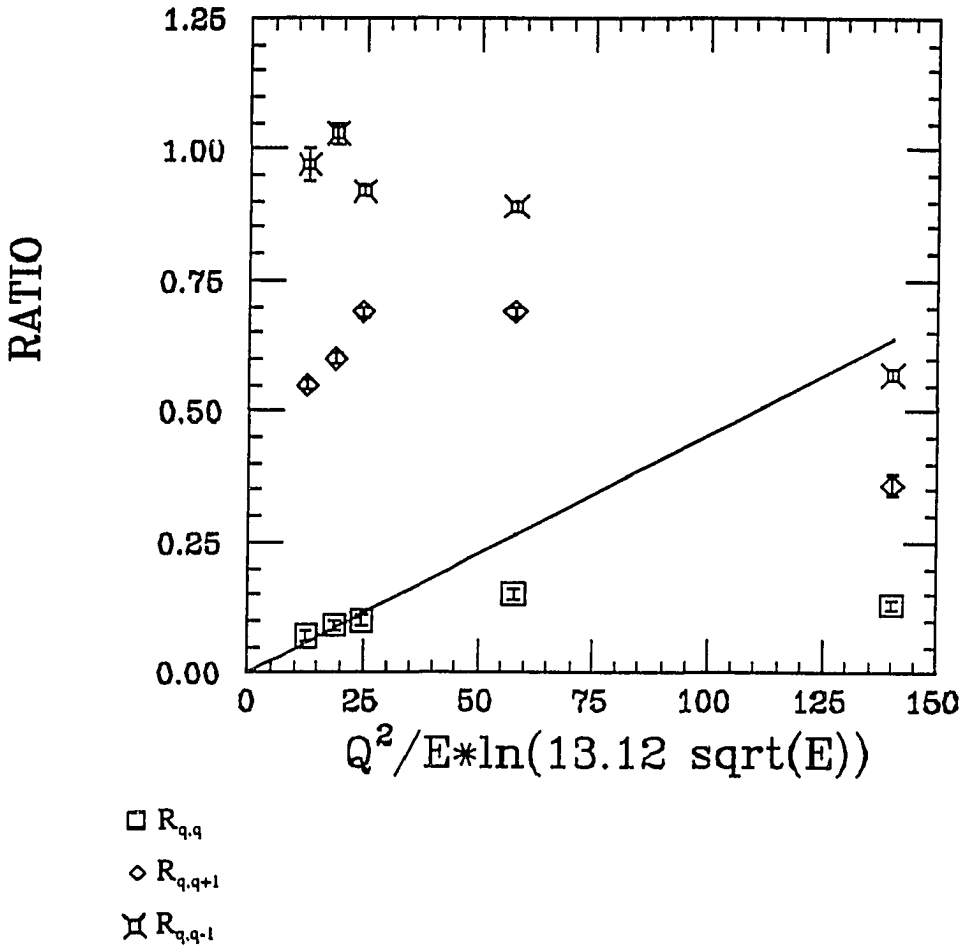

Figure 13. Ratios of Double-to-Single Ionization for S^{6+} Projectiles as a Function of the Scaling Parameter of Knudsen et al. (1984). The solid line represents the scaling of Knudsen et al. (1984) given by Eq. 8.

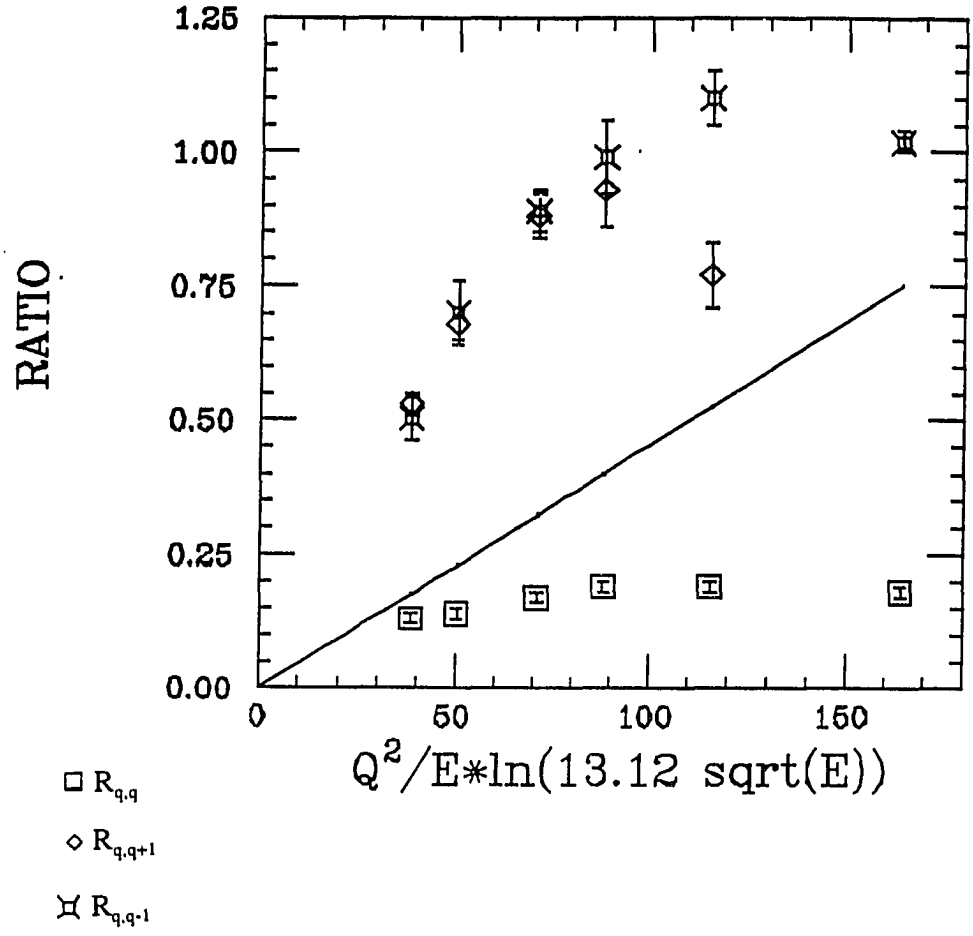

Figure 14. Ratios of Double-to-Single Ionization for S^{13+} Projectiles as a Function of the Scaling Parameter of Knudsen et al. (1984). The solid line represents the scaling of Knudsen et al. (1984) given by Eq. 8.

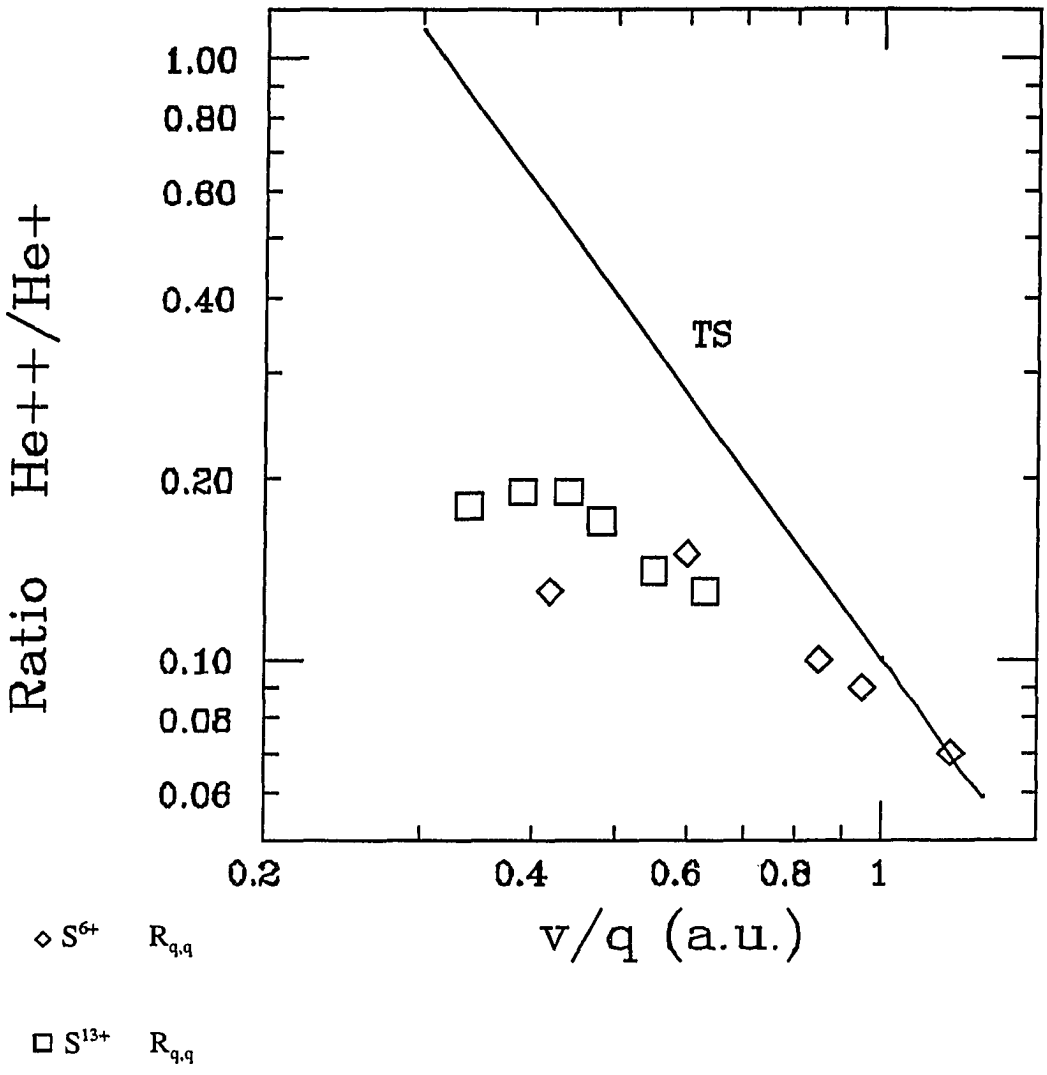

Figure 15. Ratios of Double-to-Single Ionization of Helium as a Function of Velocity (in a.u.) Divided by Charge. The TS line denotes the v^{-2} velocity dependence of the two-step mechanism.

The two-step mechanism is expected to dominate when $q/v > 0.2$, while shake-off dominates for $q/v << 1.0$ (Tanis et al., 1992). However, it should be noted that first-order perturbation theory was used in the development of the two-step mechanism (McGuire, 1982), and this restricts the region which exhibits a $(v/q)^{-2}$ dependence to $v/q = 1\text{-}5$. Thus, it is evident that the S^{13+} data lie outside the perturbative two-step regime and do not exhibit the predicted $(v/q)^{-2}$ behavior. For S^{6+}, the two highest energy points correspond to $v/q = 1.0$ and 1.1 respectively. These points fall just within the limits of the perturbative regime. The 20 MeV point with $v/q = 0.83$ lies just outside the perturbative regime while the points at 5 and 10 MeV are beyond where the perturbative treatment for the two-step mechanism is valid. This is displayed in Figure 15 where the highest-velocity points approach a $(v/q)^{-2}$ dependence, but deviate significantly at lower velocities.

Plotted in Figure 16 are ratios for S^{6+} along with O^{6+}. The O^{6+} data are from Tanis et al. (1991). The oxygen data are within the perturbative two-step regime and exhibit an R dependence similar to S^{6+}. This indicates that for pure target ionization the ratio of double-to-single ionization is independent of the projectile species (S^{6+} or O^{6+}) and depends only on the charge of the ion. This similarity between oxygen and sulfur is not observed, however, for ionization accompanied by projectile electron capture or loss.

Coincidence Cross Sections

Coincidence cross sections were determined for the processes of pure target

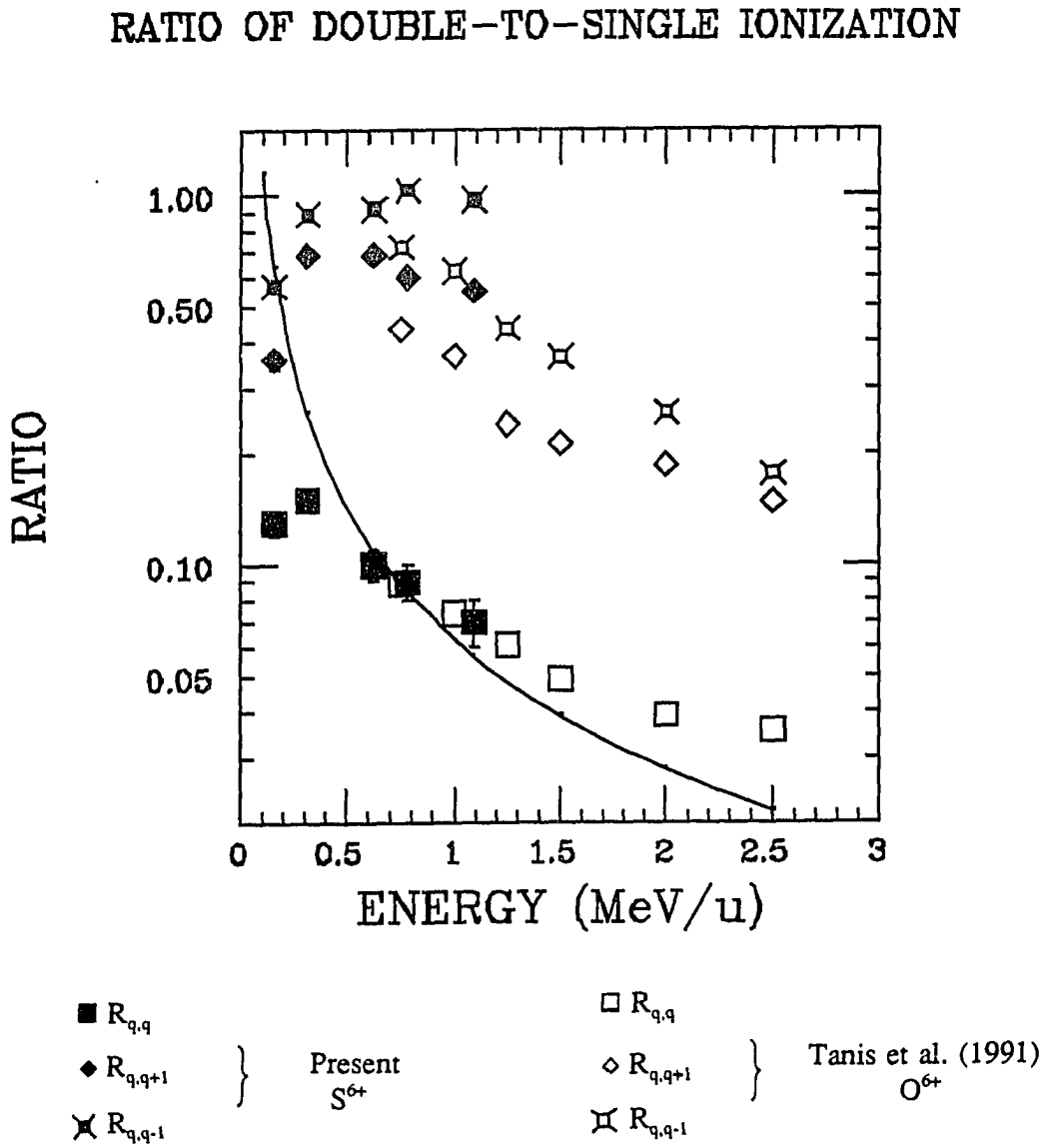

Figure 16. Ratios of Double-to-Single Ionization of He for S^{6+} and O^{6+} Projectiles as a Function of Energy. The O^{6+} data are from Tanis et al. (1991).

ionization, target ionization associated with single-electron capture, and target ionization associated with single-electron loss by the projectile. If we consider the total single-electron capture cross section, then from charge conservation

$$\sigma_{q,q-1} = \sigma^{01}_{q,q-1} + \sigma^{02}_{q,q-1} \tag{13}$$

which gives

$$\sigma^{01}_{q,q-1} = \frac{\sigma_{q,q-1}}{1+R} \tag{14}$$

and

$$\sigma^{02}_{q,q-1} = \sigma_{q,q-1}\frac{R}{1+R} \tag{15}$$

with

$$R = \frac{\sigma^{02}_{q,q-1}}{\sigma^{01}_{q,q-1}}.$$

That is, the sum of the pure single-capture cross section $(\sigma^{01}_{q,q-1})$ and the transfer ionization cross section $(\sigma^{02}_{q,q-1})$ must equal the total one-electron transfer cross section. Once the singles cross sections $(\sigma_{q,q-1})$ and the ratios (R) are known, these values can be used to determine $\sigma^{01}_{q,q-1}$ and $\sigma^{02}_{q,q-1}$ and then from Eq. (12), the recoil ion detector efficiency can be determined and, in turn, the partial cross sections for the processes of pure ionization and single-electron loss in coincidence with single and double ionization of the helium target.

The coincidence cross sections for S^{6+} and S^{13+} are listed in Tables 3, 4, and 5, along with their associated statistical errors. Plotted in Figs. 17 and 18 are the coincidence cross sections as a function of energy. It is obvious that for both

Table 3

Cross Sections for Single and Double Ionization of Helium Coincident With Single-Electron Capture by S^{6+} and S^{13+} Ions

E (MeV)	$\sigma_{q,q-1}^{01}$ (cm^2)	$\sigma_{q,q-1}^{02}$ (cm^2)
	q = 6+	
10	(3.5 ± 0.4) [-17]	(3.2 ± 0.1) [-17]
20	(2.6 ± 0.3) [-18]	(2.5 ± 0.4) [-18]
25	(1.2 ± 0.1) [-18]	(1.3 ± 0.1) [-18]
35	(3.3 ± 0.4) [-19]	(3.2 ± 0.5) [-19]
	q = 13+	
15	(9.6 ± 1.0) [-17]	(9.6 ± 1.0) [-17]
20	(4.4 ± 0.5) [-17]	(4.9 ± 0.6) [-17]
25	(2.1 ± 0.3) [-17]	(2.1 ± 0.3) [-17]
30	(1.1 ± 0.1) [-17]	(9.7 ± 1.2) [-18]
40	(3.5 ± 0.5) [-18]	(2.5 ± 0.4) [-18]
50	(1.6 ± 0.2) [-18]	(8.0 ± 1.3) [-19]

Table 4

Cross Sections for Single and Double Ionization of Helium Coincident With Single-Electron Loss by S^{6+} and S^{13+} Ions

E (MeV)	$\sigma_{q,q+1}^{01}$ (cm^2)	$\sigma_{q,q+1}^{02}$ (cm^2)
	q = 6+	
10	(9.6 ± 3.3) [-18]	(6.7 ± 2.5) [-18]
20	(8.4 ± 1.0) [-18]	(5.8 ± 0.8) [-18]
25	(9.9 ± 1.0) [-18]	(5.8 ± 0.6) [-18]
35	(7.8 ± 1.2) [-18]	(4.3 ± 0.7) [-18]
	q = 13+	
15	(7.9 ± 2.1) [-20]	
20	(1.5 ± 0.3) [-19]	(1.1 ± 0.2) [-19]
25	(2.0 ± 0.3) [-19]	(1.9 ± 0.4) [-19]
30	(2.5 ± 0.3) [-19]	(2.1 ± 0.3) [-19]
40	(2.9 ± 0.4) [-19]	(2.0 ± 0.3) [-19]
50	(2.3 ± 0.3) [-19]	(1.2 ± 0.2) [-19]

Table 5

Cross Sections for Single and Double Ionization of Helium Coincident With No Charge Change by S^{6+} and S^{13+} Ions

E (MeV)	$\sigma_{q,q}^{01}$ (cm^2)	$\sigma_{q,q}^{02}$ (cm^2)
	q = 6+	
10	(8.5 ± 1.6) [-16]	(1.3 ± 0.2) [-16]
20	(5.0 ± 0.5) [-16]	(5.0 ± 0.6) [-17]
25	(5.1 ± 0.5) [-16]	(4.6 ± 0.5) [-17]
35	(4.2 ± 0.6) [-16]	(3.1 ± 0.4) [-17]
	q = 13+	
15	(8.0 ± 0.8) [-16]	(1.4 ± 0.2) [-16]
20	(9.4 ± 1.1) [-16]	(1.7 ± 0.2) [-16]
25	(8.7 ± 1.1) [-16]	(1.7 ± 0.3) [-16]
30	(7.3 ± 0.9) [-16]	(1.3 ± 0.2) [-16]
40	(5.9 ± 0.9) [-16]	(8.4 ± 1.2) [-17]
50	(3.8 ± 0.6) [-16]	(4.8 ± 0.7) [-17]

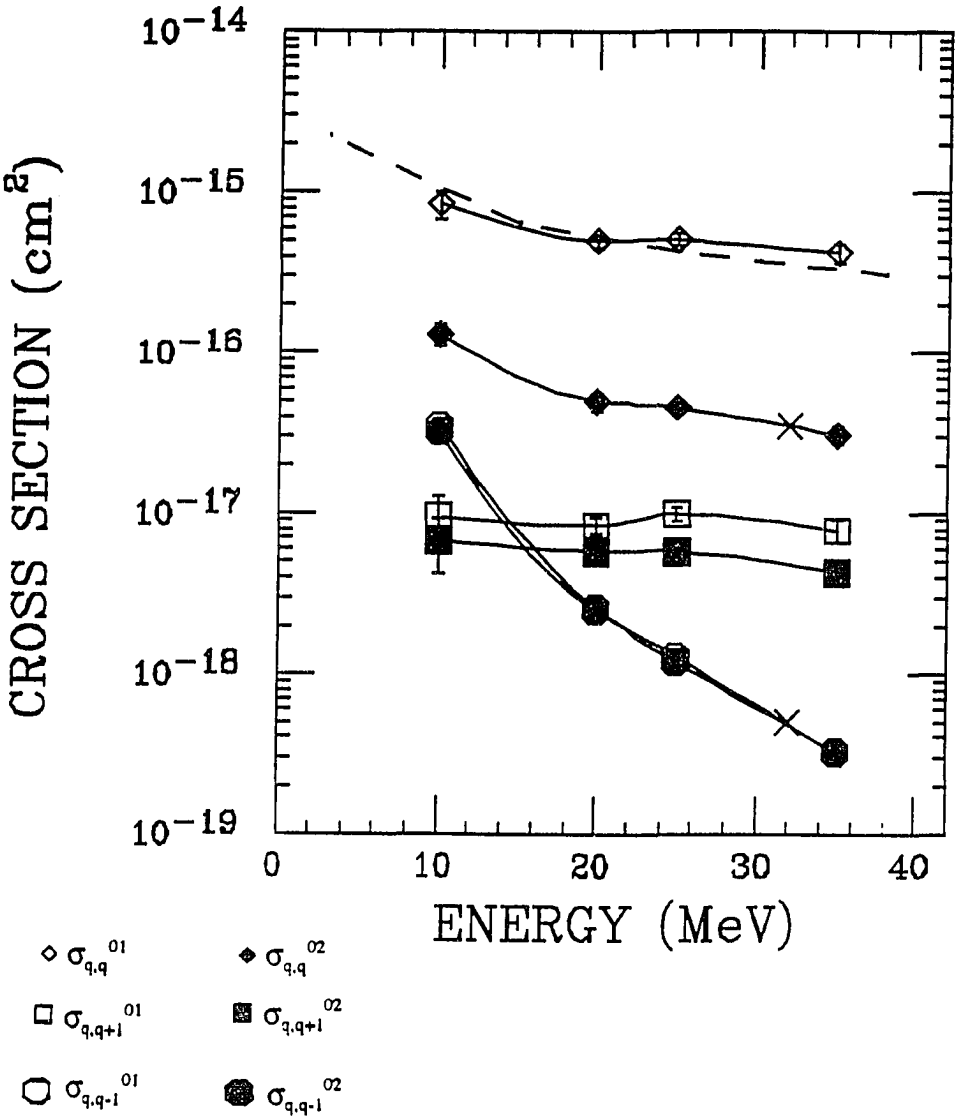

Figure 17. Cross Sections for S^{6+} Incident on He. The dashed curve represents the scaling of McKenzie and Olson (1987). The other lines are drawn to guide the eye. The points labeled by X were obtained from the theoretical curves of McKenzie and Olson and the upper one is for pure double ionization while the lower one is for transfer ionization.

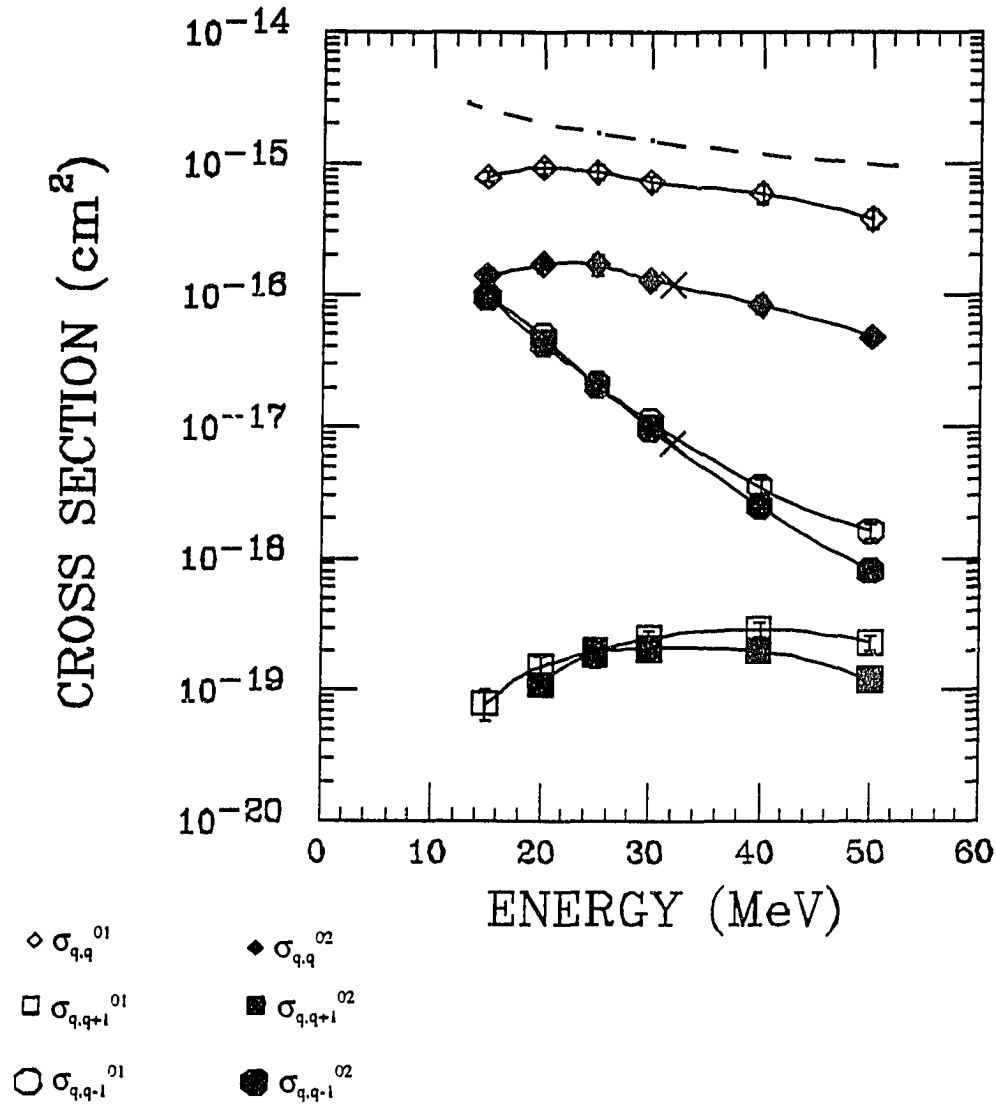

Figure 18. Cross Sections for S^{13+} Incident on He. The dashed curve represents the scaling of McKenzie and Olson (1987). The other lines are drawn to guide the eye. The points labeled by X were obtained from the theoretical curves of McKenzie and Olson and the upper one is for pure double ionization while the lower one is for transfer ionization.

charge states the pure ionization process is dominant. Thus, as expected, single and double ionization is most probable when the projectile does not change charge state. For S^{6+} and S^{13+}, the pure ionization cross sections all decrease with increasing energy except for the lowest energy data point for q = 13+. The dashed curve is based on the theory of McKenzie and Olson (1987) which gives the pure ionization cross section as

$$\sigma_{q,q}^{01} = 1.46\times10^{-17}\frac{q^{1.78}}{E^{0.78}} \quad cm^2$$

where q is the charge of the projectile and E is the energy in MeV/u. For the energy range considered, the q = 6+ data are in good agreement with McKenzie and Olson (1987) while the q = 13+ data all fall slightly beneath the curve.

Also shown in Figs. 17 and 18 are the cross sections for target ionization associated with projectile electron capture and loss. The coincidence cross sections for single ionization associated with single-electron loss from the projectile are slightly larger than the cross sections for double ionization associated with single-electron loss and the cross sections for both charge states show a rather weak velocity dependence. Ionization associated with capture for both S^{6+} and S^{13+} decreases with velocity by about two orders of magnitude over the energy range investigated, with the cross sections for S^{13+} being somewhat larger as expected due to the larger charge. Also shown on the graph are theoretical points for double ionization and transfer ionization at 32 MeV (1 MeV/u). These points were obtained from the theoretical curves of McKenzie and Olson (1987), and show

good agreement with the experimental data.

CHAPTER V

CONCLUSION

In summary, cross sections for the processes of pure ionization, ionization associated with capture, and ionization associated with single loss by $S^{6,13+}$ projectiles incident on helium have been experimentally determined. For the collision systems considered here, the projectile velocity range was 0.16-1.6 Mev/u. These cross sections were determined by associating projectile ions with recoiling helium target ions using standard coincidence techniques. Total one-electron transfer and loss cross sections were also measured. These cross sections were compared to previous results and theories as well as with the empirical scaling rule of Schlachter et al. (1987).

The ratio of double-to-single ionization of helium was determined. For pure ionization, only the q = 6+ charge state at the highest energies investigated scales as $(v/q)^{-2}$. The S^{13+} v/q range is outside the region where the perturbation theory used to develop the two-step mechanism is valid. The pure ionization ratios for S^{13+} show substantial deviations from the theory and do not exhibit a simple $(v/q)^{-2}$ dependence. Furthermore, it is found that the ratio of double-to-single ionization becomes significantly enhanced when the projectile ion captures or loses an electron. These ratios were compared with those obtained in a similar collision

system involving O^{6+} projectiles (Tanis et al., 1991). For both projectiles (O^{6+} and S^{6+}), the pure ionization ratios exhibited the scaling properties predicted by Knudsen et al. (1984), and were independent of the projectile species.

In conclusion, the double ionization of helium by highly charged sulfur projectiles was investigated. For the velocity regime considered here, double ionization for S^{13+} on He can not be adequately described by the existing perturbative theory. Thus, more sophisticated theories must be developed to accurately describe the double ionization of helium by S^{13+} in the non-perturbative two-step regime.

BIBLIOGRAPHY

Choi, B.H., Merzbacher, E., & Khandelwal, G.S. (1973). Tables for Born approximation calculations of L-sub-shell ionization by simple heavy charged particles. Atomic Data, 5, 291-294.

Clark, M.W., Bernstein, E.M., Tanis, J.A., Graham, W.G., McFarland, R.H., Morgan, T.J., Johnson, B.M., Jones, K.W., & Meron, M. (1986). Electron capture and loss for 2.5-200 MeV $_{16}S^{13+}$ + He collisions. Physical Review A, 33, 762.

Gilbody, H.B. (1979). Atomic collision processes in controlled thermonuclear fusion research. Advances in Atomic and Molecular Physics, 15, 293.

Harrison, M.F.A. (1978). The role of atomic and molecular processes in fusion research. Physics Reports, 37, 59.

Heber, O., Bandong, B.B., Sampoll, G., & Watson, R.L. (1990). Double and single ionization of helium by high-velocity N^{7+} ions. Physical Review Letters, 64, 851.

Hogan, J.T. (1978). Atomic and molecular data needs, priorities, and accuracies for tokamak beam injection. Physics Reports, 37, 83.

Inokuti, M. (1971). Inelastic collisions of fast charged particles with atoms and molecules—the Beth theory revisited. Review of Modern Physics, 43, 297.

Janev, R.K. (1989). Atomic physics in fusion developement. Bulletin of the International Atomic Energy Agency, 31, 28.

Knudsen, H., Andersen, L.H., Hvelplund, P., Astner, G., Cederquist, H., Danared, H., Liljeby, L., & Rensfelt, K-G. (1984). An experimental investigation of double ionization of helium atoms in collisions with fast, fully stripped ions. Journal of Physics B, 17, 3545.

Madison, D.H., & Merzbacher, E. Theory of charged-particle excitation. In B. Crasemenn (Ed.), Atomic Inner Shell Processes (pp. 1-72). New York: Academic.

McGuire, J.H. (1982). Double ionization of helium by protons and electrons at high velocities. Physical Review Letters, 49, 1153.

McGuire, J.H. (1984). High-velocity limits for the ratio of double to single ionization by charged particles and by photons. Journal of Physics B, 17, L779.

McGuire, J.H., Muller, A., Schuch, B., Groh, W., & Salzborn, E. (1987). Ionization of helium by highly charged ions at 1.4 MeV/amu. Physical Review A, 35, 2479.

McGuire, J.H., & Weaver, O.L. (1977). Independent electron approximation for atomic scattering by heavy particles. Physical Review A, 16, 41.

McKenzie, M.L., & Olson, R.E. (1987). Ionization and charge exchange in multiply-charged-ion-helium collisions at intermediate energies. Physical Review, 35, 2863.

Schlachter, A.S., Steams, J.W., Berkner, K.H., Stockli, M.P., Graham, W.G., Bernstein, E.M., Clark, M.W., & Tanis, J.A. (1987). Electron capture for fast highly charged ions in He: An empirical scaling rule revisited. In XV International Conference on the Physics of Electronic and Atomic Collision, (pp. 505-506). Belfast, United Kingdom: International ICPEAC organization.

Shah, M.B., & Gilbody, H.B. (1981). Experimental study of the ionization of atomic hydrogen by fast H^+ and He^{2+} ions. Journal of Physics B, 14, 2361.

Tanis, J.A., Bernstein, E.M., Clark, M.W., Ferguson, S.M., & Price, R.N. (1991). Target ionization accompanied by projectile electron loss in fast $O^{6,7+}$ + He collisions. Physical Review A, 43, 4723.

Tanis, J.A., DuBois, R.D., & Schlachter, A.S. (1992). Comment on "Double and Single Ionization of Helium by High-Velocity N^{7+} Ions" Physical Review Letters, 68, 897.